LETTER

On freshwater fluxes and the Atlantic meridional overturning circulation

B. B. Cael ⬤,[1]* *Malte F. Jansen*[2]
[1]National Oceanography Centre, Southampton, SO14 3ZH, UK; [2]Department of the Geophysical Sciences, University of Chicago, 5734 S Ellis Ave, Chicago, IL 60637, USA

Scientific Significance Statement

In the North Atlantic, warm surface waters flow northward, cool and sink at high latitudes, then travel southward in the deep ocean. This "overturning" circulation carries a tremendous amount of heat from the tropics to higher latitudes and influences Europe's climate. It is commonly thought that the exchange of water between the atmosphere and the surface ocean via evaporation and precipitation serves as a brake on the overturning. By using physical reasoning and computer simulations of virtual oceans with more/less evaporation and precipitation, we argue that in the modern ocean, this exchange of water with the atmosphere actually strengthens the overturning. These results may therefore have implications for our understanding of this important component of the ocean circulation and its relationship with the atmosphere.

Abstract

We address the role of freshwater forcing in the modern day ocean. Specifically, we ask the question of whether an amplification of the global freshwater forcing pattern leads to a strengthening or weakening of the steady-state Atlantic Meridional Overturning Circulation (AMOC). While the role of freshwater forcing in the AMOC has received much attention, this question remains unresolved, in part because past studies have primarily investigated idealized models, large regime shifts away from the modern ocean state, or coupled atmosphere–ocean simulations on shorter timescales than required for the deep ocean to equilibrate. Here we study the AMOC's sensitivity at equilibrium to small perturbations in the magnitude of the global freshwater fluxes in simulations performed with a realistically configured ocean circulation model. Our results robustly suggest that for the equilibrium state of the modern ocean, freshwater fluxes strengthen the AMOC, in the sense that an amplification of the existing freshwater flux-forcing pattern leads to a strengthening of the AMOC and vice versa. A simple physical argument explains these results: the North Atlantic is anomalously salty at depth and increased freshwater fluxes act to amplify that salinity pattern, resulting in enhanced AMOC transport.

In the northern Atlantic, cold-water masses form and sink before flowing southward at depth. The water rises back up in the Pacific and Southern Oceans and returns to the northern Atlantic in the upper ocean (Lumpkin and Speer 2007; Marshall and Speer 2012; Talley 2013). This pathway is referred to as the Atlantic Meridional Overturning Circulation (AMOC). The AMOC is a principal object of study in physical oceanography because it plays a disproportionate role in Northern Hemisphere climate, meridional heat transport, the sequestration of heat anomalies into the ocean interior, the ventilation of the deep ocean, and the connection of the ocean between the Northern and Southern hemisphere, among other things (Buckley and Marshall 2016, and references therein).

Our contemporary understanding of the AMOC suggests that the buoyancy contrast between the North Atlantic deep-water

formation region and other parts of the ocean is one of the important factors that determine the strength (magnitude of transport) of the AMOC (Welander 1971; Gnanadesikan 1999; Nikurashin and Vallis 2012; Wolfe and Cessi 2014). Although there is not a consensus about what exact buoyancy contrast is most relevant, an increase in the density of North Atlantic Deep Water (NADW) is generally assumed to lead to a strengthening of the AMOC.

The buoyancy pattern of the ocean is driven in parts by atmospheric freshwater fluxes (evaporation and precipitation) and these fluxes are therefore believed to influence the AMOC. A formative paper by Stommel (1961) exploring the dynamics of an idealized two-vessel system suggested, along with the possibility of multiple stable states for the AMOC, contrasting roles of temperature and freshwater forcing on the AMOC. Specifically, heat exchange with the atmosphere was argued to amplify the overturning circulation, while freshwater exchange inhibits it. Stommel was the first to note the highly idealized character and therefore limited applicability of his model to the ocean (Stommel 1961), and its usefulness has been questioned by many others since (Straub 1996; Wunsch 2005). Rather than digging deeply into the dynamical and energetic inconsistencies of the Stommel model that have been discussed in previous work, we will here focus on one key qualitative difference between the Stommel model and the ocean. Figure 1 shows that waters in the subsurface of the northern Atlantic, where NADW is formed, are saltier than almost all of the rest of the ocean below the subtropical thermocline. Therefore, the salinity pattern *increases* the buoyancy contrast between these convective waters and most of the rest of the deep ocean—which is the opposite of Stommel's picture where the northern sinking box was assumed to be relatively fresh.

Since Stommel (1961), the influence of freshwater fluxes in the AMOC has become the subject of considerable research. While the view that freshwater fluxes weaken the AMOC widely prevails (Weaver et al. 1993; Marotzke 1994; Rahmstorf 1996; Nilsson and Walin 2001; Stouffer et al. 2006), a number of studies have also pointed toward the possibility of a strengthening of the AMOC under increased freshwater forcing (Klinger and Marotzke, 1999; Wang et al. 1999; Nilsson and Walin 2001; Latif 2000; Thorpe et al. 2001). The existing studies differ substantially in the types of models that are being considered, and the experiments that are performed. A number of studies consider centennial time-scale coupled climate simulations of global warming, where the ocean's boundary conditions change in a myriad of ways, and the deep ocean is not in equilibrium (Latif 2000; Thorpe et al. 2001; Stouffer et al. 2006). Others consider idealized models (Rooth 1982; Welander 1986; Weaver et al. 1993; Klinger and Marotzke, 1999; Wang et al. 1999; Nilsson and Walin 2001), or past climates (Bice and Marotzke 2001), which can provide mechanistic insights, but may not adequately represent the important roles of basin geometry and asymmetric evaporation minus precipitation patterns for Earth's present-day ocean (Ferreira et al. 2018). The widely different
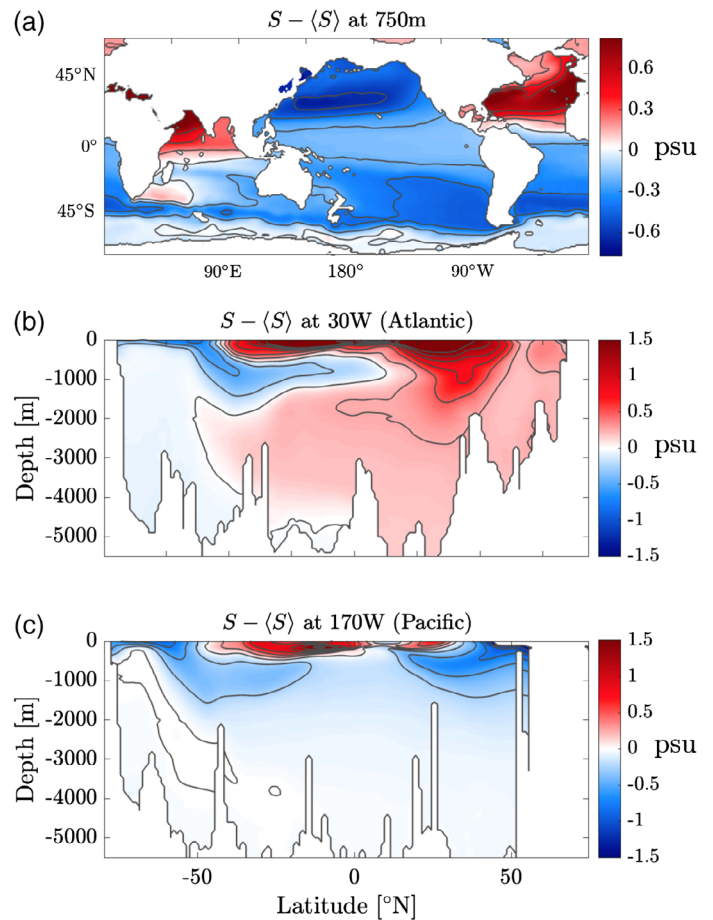

Fig. 1. (a) Salinity at 750 m depth [averaged 1955–2012, from the World Ocean Atlas version 2 (Zweng et al. 2013)], relative to the global mean. At this depth, the northern Atlantic is saltier than all of the Pacific, Southern, and South Atlantic oceans. The depth of 750 m was chosen to characterize the ocean's structure below the thermocline; the general pattern is not sensitive to this specific choice. (b, c) Depth-latitude sections of salinity in the (b) Atlantic (30°W) and (c) Pacific (170°W). The sections further highlight the high salinity of NADW relative to other deep and intermediate water masses.

model setups and various additional factors that come into play in coupled climate simulations complicate the interpretation of the results and may explain the differing conclusions drawn by previous authors.

Here we use numerical ocean general circulation model (GCM) simulations with present-day continental configuration and freshwater forcing to investigate the question: "does the modern freshwater forcing pattern act to strengthen or weaken the strength of the AMOC?" Specifically, we consider the response of the equilibrium AMOC strength to a small amplification or weakening of the existing freshwater forcing pattern. We hypothesize that an amplification of the forcing pattern strengthens the modern AMOC, because (1) the northern Atlantic is anomalously salty at depth, suggesting that the existing salinity pattern likely acts to amplify the strength of the

AMOC, and (2) enhanced freshwater forcing is likely to enhance the existing salinity pattern because freshwater fluxes to zeroth order act to generate salinity differences (Cullum et al. 2016; Cael and Ferrari 2017; below).

Whether the existing salinity pattern amplifies or weakens the AMOC depends on what is the most relevant buoyancy contrast, δb, to determine AMOC strength. Dynamical arguments for the strength of a diffusive overturning go back to Welander (1971) whose model suggests that the relevant buoyancy contrast is between NADW and the low latitude lower thermocline, where waters are upwelling diffusively. For an adiabatic pole-to-pole circulation, the relevant buoyancy contrast instead has been described as that between NADW and the lightest waters at the northern flank of the Antarctic Circumpolar Current (Gnanadesikan 1999; Nikurashin and Vallis 2012; Wolfe and Cessi 2014). As the latter water mass flows northward in the basin under the tropical thermocline, both arguments crudely suggest a δb related to the contrast between NADW and the lower thermocline or intermediate waters in the basin. Other studies have argued that AMOC strength is affected by a competition between different deep ocean water masses (Klinger and Marotzke 1999). While the relevant salinity contrast depends on the exact definitions used, Fig. 1 shows that subsurface waters in the north Atlantic are saltier than almost any water mass below the tropical thermocline, suggesting that the present-day salinity pattern is likely to amplify the overturning circulation.

We expect an amplification of the existing salinity pattern under amplified freshwater forcing based on the steady state salinity budget:

$$\mathrm{Adv}(\mathbf{u}, S) + \mathrm{Diff}(S) = F \tag{1}$$

where $\mathrm{Adv}(\mathbf{u}, S)$ is a bilinear advection operator, $\mathrm{Diff}(S)$ is a linear diffusion operator, and F denotes the surface salinity forcing. If we amplify or weaken forcing by multiplying F with a factor $1 + \epsilon$, we can obtain an equation for the perturbed fields as

$$\mathrm{Adv}(\mathbf{u}_0, \Delta S) + \mathrm{Diff}(\Delta S) + \mathrm{Adv}(\mathbf{\Delta u}, S) = \epsilon F_0 \tag{2}$$

where $S = S_0 + \Delta S$, $\mathbf{u} = \mathbf{u_0} + \mathbf{\Delta u}$, and $F = (1 + \epsilon)F_0$, with u_0, S_0 and F_0 denoting the unperturbed velocity, salinity, and forcing fields, respectively. The first two terms on the left-hand side describe the passive response of the salinity field to a change in the forcing, while the last term describes a salt advection feedback associated with changes in the circulation (which includes both a linear and nonlinear component). Considering the passive response only (i.e., eliminating, for now, the feedback term), and comparing Eqs. (1) and (2), we find a solution for the salinity anomaly of the form

$$\Delta S = \epsilon S_0 + \mathrm{const.} = \epsilon(S_0 - \langle S_0 \rangle) \tag{3}$$

where $\langle S_0 \rangle$ is the global mean salinity, which remains constant as long as F integrates to zero. The salinity response to amplified freshwater forcing is then simply an amplification

of the existing pattern. The salinity advection feedback will modify this response, but as the circulation change is to first order driven by the salinity anomaly itself, we expect a quantitative modification rather than a change in the sign of the large-scale response pattern. Thus, if (1) the present-day salinity pattern tends to amplify the buoyancy contrast most relevant in determining the strength of the AMOC, and (2) enhanced freshwater forcing amplifies the existing salinity pattern, we expect that in present-day conditions enhanced freshwater forcing acts to strengthen the AMOC. The simulations described later robustly corroborate this hypothesis.

Methods

We conducted numerical simulations using the Massachusetts Institute of Technology general circulation model (Marshall et al. 1997) in a global rigid lid configuration at $2.8°$ horizontal resolution with 15 nonuniform vertical levels. Configuration specifics can be found in the supplementary material. All simulations described later are run for 10,000 yr, and diagnostics are then computed for the last century of model output (centennial-scale variability in the model is negligible after >9000 yr of model run time). As we are interested in the long-timescale response, we use a coarse-grained model grid in order to be able to run the simulations for millenia so as to ensure they reach equilibrium.

Atmospheric freshwater fluxes are modeled as a salt flux boundary condition. Salt fluxes are based on an annually averaged climatology of evaporation-precipitation-runoff synthesized from observations (Jiang et al. 1999; Supporting Information Fig. S1) to which a small global correction has been applied to ensure global freshwater flux balance, and freshwater fluxes are converted to salt fluxes using a mean ocean salinity of 35 psu. The total surface freshwater flux integrated over the Atlantic basin (between $35°$S and $60°$N) amounts to a net evaporation of about 0.75 Sv, which is at the upper end of a number of recent estimates (Craig et al. 2017). The effect of a potential bias in the freshwater flux over the Atlantic will be discussed in Section 4.

We perform seven total simulations, which differ only in the amplitude of their freshwater forcing boundary conditions. To test the sensitivity of our results to the type of boundary condition imposed, we also perform a second set of simulations that are identical to these except that the climatological freshwater fluxes are complemented by a relaxation to the climatological sea surface salinity (SSS) (Levitus and Boyer 1994a) with a piston velocity of 28 cm d^{-1}. The simulations with SSS restoring echo the results of our primary simulations, and we will hence focus our discussion on the latter. Results for the simulations with salinity restoring are included in the SM and are discussed in the main text wherever noteworthy differences exist.

To quantify the AMOC in the simulations, we introduce the overturning stream function (Ψ), in units of Sverdrups
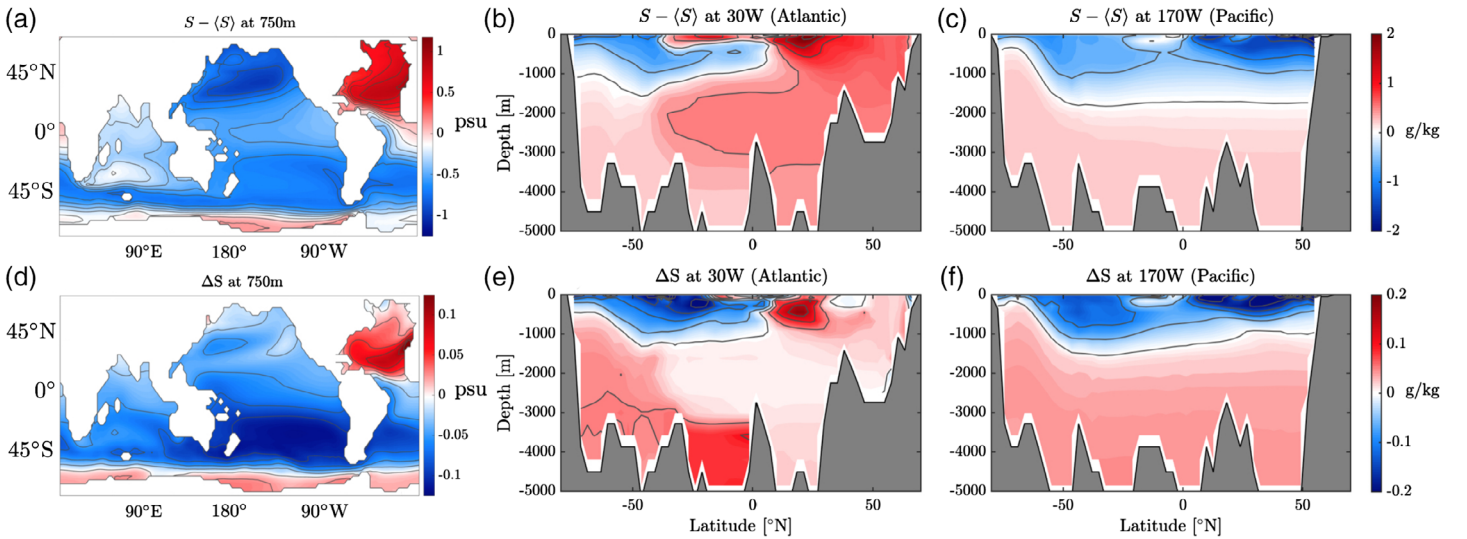
Fig. 2. (a, b, c) As Fig. 1, but for the control climate of the GCM simulation. (d, e, f) corresponding changes in salinity in the simulation with +2 K equivalent freshwater forcing, relative to the reference case.

(1 Sv = 10^6 m³/s), which represents the Atlantic's zonally integrated net volume transport. Here Ψ is defined to be the zonally integrated transport of water above the potential density surface ϱ, which is mapped into physical space using the time and zonal mean potential density field (Döös and Webb 1994; SM). We also compute the depth-averaged streamfunction Ψ^z, defined to be the zonally integrated transport of water above a constant depth z; in the main text we focus on Ψ, but our conclusions hold similarly for Ψ^z (SM). The positive maxima of Ψ and Ψ^z serve as metrics for the strength of the AMOC. We define $\Psi_{max}^{(z)} \equiv \max\left[\Psi^{(z)}\right]$, $\Psi_0^{(z)} \equiv \max\left[\Psi^{(z)}(y=0°\mathrm{N})\right]$, and $\Psi_{30}^{(z)} \equiv \max\left[\Psi^{(z)}(y=30°\mathrm{N})\right]$ to quantify the maximum strength of the AMOC and its strength at the equator and in the subtropics, respectively.

The equilibrium state of the reference simulations (using the default freshwater flux field and in the restoring case the default SSS field) largely reproduce the large-scale subsurface salinity structure and time-mean circulation patterns of the present-day ocean, with comparable AMOC, vertical structure, midlatitude gyres, and Antarctic Circumpolar Current (Wunsch 2014; Talley 2013; Cael and Ferrari 2017; Lauderdale 2010; Figs. 2 and 3). For the subsurface salinity, some differences exist, most notably in the Indian Ocean and the Pacific's upper thermocline, and the AMOC is a few Sv stronger than observations. For the simulation with restoring these salinity biases are reduced and the AMOC magnitude is comparable to observations.

We also perform six simulations with perturbed freshwater fluxes relative to the reference simulation. Following Held and Soden (2006), we apply a multiplicative factor to the surface freshwater fluxes of $1.07^{\Delta T_{equiv.}}$, where $\Delta T_{equiv.}$ is a hypothetical global mean surface temperature change and the 7% is based
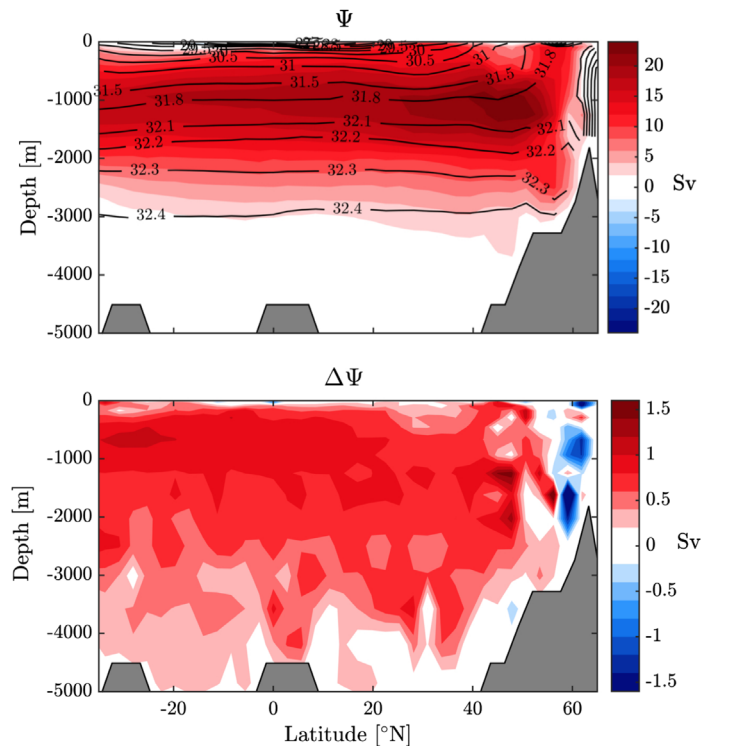

Fig. 3. (a) Isopycnally averaged meridional overturning streamfunction, Ψ (colors, contour interval: 2 Sv), and zonally averaged potential density referenced to 1 km depth, σ_1 (black lines), for the reference (0 K-equivalent) simulation. The isopycnally averaged overturning streamfunction has been mapped back to physical space using the zonal mean potential density field. See Methods for description of simulations and Ψ. (b) Difference in Ψ between the +2 K-equivalent and control simulation (contour interval: 0.2 Sv). Ψ increases throughout most of the Atlantic, and NADW formation moves southward.

on a Clausius-Clapeyron scaling whereby the global hydrological cycle is amplified/reduced by ∼7% per 1 K increase/decrease in global mean surface temperature (Held and Soden 2006; Durack et al. 2012). In the simulations with SSS restoring a similar factor is also applied to the anomalies relative to the global mean of the SSS relaxation field. We use $\Delta T_{equiv.}$ values of ± 1, ± 2, and ± 5 K, thereby including both small perturbations, to which mostly linear responses are expected, and comparatively large perturbations, which are more likely to induce complex nonlinear readjustments of the circulation. We focus on robust, qualitative responses because the AMOC is a complex residual circulation, implying that feedbacks and other details neglected by our simple argument are likely to affect the quantitative results.

Results

The simulations bear out the hypothesis that, broadly speaking, an amplification of the freshwater forcing pattern should strengthen the AMOC via amplifying the positive subsurface salinity anomaly in the northern Atlantic. Figures 2 and 3 illustrate this for the +2 K-equivalent simulation. Fig. 2 shows that the change in salinity between the +2 K-equivalent simulation and the reference case largely coincides with the salinity anomalies of the reference simulation, meaning that "the salty get saltier and the fresh get fresher" (Held and Soden 2006; Durack et al. 2012). Thus the salinity contrast between the anomalously salty northern Atlantic and most of the rest of the ocean is increased, which is expected to amplify the AMOC if the buoyancy contrast determines AMOC strength (Gnanadesikan 1999; Nikurashin and Vallis 2012; Wolfe and Cessi 2014), largely independently of how the relevant buoyancy contrast is defined. Figure 3 illustrates this enhancement in the overturning; the AMOC strengthens throughout the Atlantic south of ∼55°N in the +2°K-equivalent simulation.

Though the general pattern of amplification appears robust, some noteworthy differences exist between the salinity pattern of the reference climate vs. the response to amplified freshwater forcing. First, the +2°K-equivalent simulation shows a somewhat more pronounced salinification of the Southern Ocean around Antarctica and associated increase in salinity throughout the abyssal ocean, compared to what would be expected from a pure amplification of the salinity pattern in the control simulation (Fig. 2). Second, the +2°K-equivalent simulation shows little systematic change in the salinity at the highest latitudes in the north Atlantic and Labrador sea, despite an anomalously high salinity in the reference simulation. Both differences can be explained by the observed changes in the circulation. The increased salinity at high southern latitudes and in the abyss is likely a result of the strengthened and deepened AMOC, which leads to anomalous upwelling of relatively salty waters of Atlantic origin in the Southern Ocean (Fig. S2) and a net shift toward waters of north Atlantic origin in the abyss. The absence of a salinity increase at the highest latitudes

in the north Atlantic instead is likely associated with a southward shift of the NADW formation region (Fig. 3). The change in the circulation and associated salinity response in the northern North Atlantic are tightly linked via a salt advection feedback, as the circulation change leads to reduced advection of salty waters from the lower latitudes, while the resulting salinity anomaly pattern favors a southward shift of NADW formation. However, the effect is localized and does not affect the main result that amplification of the freshwater forcing pattern leads to a strengthening of the AMOC throughout almost all of the Atlantic.

The broad strengthening of the overturning circulation, with more localized changes in the specific structure, is also found for the depth-averaged overturning streamfunctions, Ψ^z, and for the simulations with SSS restoring (Figs. S3, S4). The overall strengthening of the AMOC via amplification of salinity differences is therefore likely to be relatively robust, while the more detailed changes in its spatial structure, such as the specific locations of deep-water formation, are less predictable and more likely to be model dependent.

The sensitivity of Ψ (the AMOC strength) to changes in the amplitude of freshwater fluxes across simulations is shown in Fig. 4 (also Figs. S5, S6). For the ± 1–2 K-equivalent simulations, AMOC strength increases uniformly with $\Delta T_{equiv.}$. For all metrics
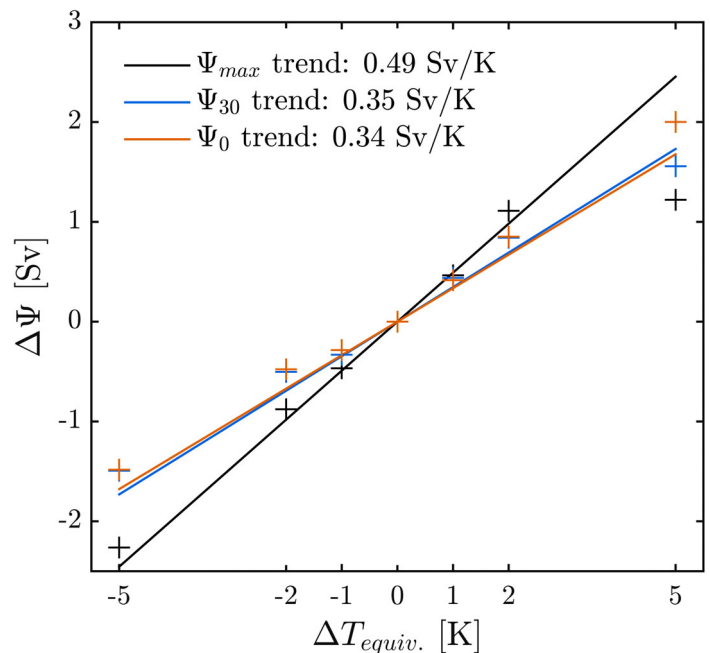

Fig. 4. Change in maxima of Ψ (the isopycnally averaged Atlantic meridional overturning streamfunction) at the equator (orange), at 30°N (blue), and the basin-wide maximum (black), vs. change in temperature-equivalent freshwater fluxes. Broadly, a strengthening of the overturning with enhanced freshwater fluxes is observed. See Methods for description of simulations and Ψ's. Regressions are forced through (0,0) and do not include ± 5 K-equivalent simulations.

(Ψ_{max}, Ψ_0, Ψ_{30}, Ψ_{max}^z, Ψ_0^z, and Ψ_{30}^z) and also for the simulations with SSS restoring, AMOC strength increases monotonically with $\Delta T_{equiv.}$, with a slope s of $0.3 < s < 0.7$ Sv/K as estimated by ordinary least squares regression of $\Delta \Psi = s \Delta T_{equiv.}$. Across the range of simulations, the strengthening of the AMOC is associated with an enhanced salinity contrast between the North Atlantic and other parts of the ocean (Figs. S7-S10). Thus, as earlier, the qualitative response is robust across all simulations and diagnostics used in this study. The magnitude of the AMOC changes is broadly consistent with scaling arguments (Gnanadesikan 1999; Nikurashin and Vallis 2012) that suggest that, all else being equal, AMOC strength is proportional to a bulk buoyancy contrast across the AMOC (SM).

While the overall strengthening of the AMOC with amplified freshwater forcing still holds for the $\pm 5^\circ$K-equivalent forcing experiment, they do not clearly follow the linear response of the smaller perturbations, suggesting that nonlinear feedbacks become increasingly important.

Discussion

Here we consider the *equilibrium* circulation of the ocean in Holocene-like geometry and atmospheric forcing, and small perturbations to this forcing. This is because we are interested in how the atmosphere affects the modern ocean on long timescales. Our results are not directly relevant for characterizing the role of atmospheric freshwater fluxes in anthropogenic climate change, as the *transient* or short-timescale response of the circulation to perturbations in the forcing often differs qualitatively from the equilibrium response (Stouffer and Manabe 2003; Jansen et al. 2018). It is also important to note that while the perturbations to freshwater fluxes that we impose are inspired by the response of the hydrological cycle to changes in global mean surface temperature (Held and Soden 2006), the temperature forcing in the model is held fixed, allowing us to isolate the effect of freshwater fluxes only. The simulated AMOC response to global warming is typically dominated by surface heat flux changes (Gregory et al. 2005).

We focus on the qualitative role of freshwater forcing in determining AMOC strength, as quantitative results are likely to be model dependent. We have used a coarse-grained model with an observation-based albeit arguably somewhat dated freshwater forcing field, which may overestimate the net evaporation over the Atlantic. The details of the freshwater forcing pattern and model resolution are likely to affect the quantitative results. However, as the model reproduces the main features of the modern ocean's salinity distribution and circulation for multiple types of boundary conditions, and the qualitative response is robust and explicable by a simple physical argument, the model is a compelling tool to illustrate the qualitative influence of atmospheric freshwater fluxes on the modern overturning.

A substantial body of literature explores the possibility of regime shifts or (bi)stability of the AMOC (Broecker et al. 1985;

Broecker 1991; Marotzke 1994; Rahmstorf 1996; Scott et al. 1999; Tziperman 2000; Stouffer et al. 2006), evincing the possibility of complex responses to large perturbations or "hosing" perturbations consistent with for example, the Greenland ice sheet collapse (where freshwater fluxes are changed in a particular location, rather than amplifying/reducing the existing forcing pattern). Previous studies have argued that a crucial factor to determine the presence of multiple equilibria in the AMOC is the sign of the basin-scale salt advection feedback (Rahmstorf 1996; Drijfhout et al. 2011; Liu et al. 2017). In Stommel's two box model, the sign of the salt advection feedback is directly related to the sign of the atmospheric freshwater forcing: A freshwater forcing that acts to increase the salinity of the northern sinking region (as we argue to be the case in the real world) would automatically be associated with northward advection of freshwater by the AMOC and hence a negative salt advection feedback. However, this relationship does not necessarily hold in the real world, where the presence of horizontal gyres, isopycnal mixing, and complex geometry complicates the picture (Longworth et al. 2005; Nilsson et al. 2013; Gent 2018; Mignac et al. 2019). The relationship between the AMOC's response to amplified freshwater forcing and the sign of the salt advection feedback therefore remains unclear, and a detailed examination of this issue is outside the scope of this study.

Conclusion

We have used numerical simulations to study the dependence of the modern overturning circulation on the amplitude of the atmospheric freshwater forcing pattern. The AMOC robustly strengthens with amplified freshwater forcing, indicating that for small perturbations around the modern state, freshwater forcing strengthens the equilibrium AMOC. We interpret this to be because NADW is saltier than almost all other deep and intermediate ocean water masses. The salinity distribution therefore contributes positively to the subsurface density contrast between the north Atlantic and the rest of the ocean, which, even though the exact relationship between the AMOC and the meridional and interbasin density gradients remains unclear, suggests that salinity contrasts act to strengthen the AMOC. An increase in the amplitude of the freshwater forcing then amplifies the existing salinity contrasts, leading to an intensification of the AMOC. Many additional feedbacks can come into play that are likely to affect the quantitative results and may even lead to a qualitatively different circulation for large enough forcing perturbations. However, the consistency between the physical argument and the simulations provides some confidence that our result is robust for small perturbations around the present-day ocean state. Repeating similar simulations with different numerical models would be informative, but in the meantime we suggest that atmospheric heat and freshwater fluxes do not compete but work together to strengthen the AMOC in the modern climate.

References

Bice, K. L., and J. Marotzke. 2001. Numerical evidence against reversed thermohaline circulation in the warm Paleocene/Eocene Ocean. J. Geophys. Res. Oceans **106**: 11529–11542. doi:10.1029/2000JC000561.

Broecker, W. S. 1991. The great ocean conveyor. Oceanography **4**: 79–89. doi:10.5670/oceanog.1991.07.

Broecker, W. S., D. M. Peteet, and D. Rind. 1985. Does the ocean-atmosphere system have more than one stable mode of operation? Nature **315**: 21–26. doi:10.1038/315021a0.

Bryan, K. 1984. Accelerating the convergence to equilibrium of ocean-climate models. J. Phys. Oceanogr. **14**: 666–673. doi:10.1175/1520-0485(1984)014<0666:ATCTEO>2.0.CO;2.

Buckley, M. W., and J. Marshall. 2016. Observations, inferences, and mechanisms of the Atlantic meridional overturning circulation: A review. Rev. Geophys. **54**: 5–63. doi:10.1002/2015RG000493.

Cael, B. B., and R. Ferrari. 2017. The ocean's saltiness and its overturning. Geophys. Res. Lett. **44**: 1886–1891. doi:10.1002/2016GL072223.

Craig, P. M., D. Ferreira, and J. Methven. 2017. The contrast between Atlantic and Pacific surface water fluxes. Tellus A: Dyn. Meteorol. Oceanogr. **69**: 1330454. doi:10.1080/16000870.2017.1330454.

Cullum, J., D. P. Stevens, and M. M. Joshi. 2016. Importance of ocean salinity for climate and habitability. Proc. Natl. Acad. Sci. **113**: 4278–4283. doi:10.1073/pnas.1522034113.

Döös, K., and D. J. Webb. 1994. The deacon cell and the other meridional cells of the Southern Ocean. J. Phys. Oceanogr. **24**: 429–442. doi:10.1175/1520-0485(1994)024<0429:TDCATO>2.0.CO;2.

Drijfhout, S. S., S. L. Weber, and E. van der Swaluw. 2011. The stability of the MOC as diagnosed from model projections for pre-industrial, present and future climates. Clim. Dyn. **37**: 1575–1586. doi:10.1007/s00382-010-0930-z.

Durack, P. J., S. E. Wijffels, and R. J. Matear. 2012. Ocean salinities reveal strong global water cycle intensification during 1950 to 2000. Science **336**: 455–458. doi:10.1126/science.1212222.

Ferreira, D., P. Cessi, H. K. Coxall, A. De Boer, H. A. Dijkstra, S. S. Drijfhout, T. Eldevik, N. Harnik, J. F. McManus, D. P. Marshall, and J. Nilsson. 2018. Atlantic-Pacific asymmetry in deep water formation. Annu. Rev. Earth Planet. Sci. **46**: 327–352. doi:10.1146/annurev-earth-082517-010045.

Gent, P. R. 2018. A commentary on the Atlantic meridional overturning circulation stability in climate models. Ocean Model. **122**: 57–66. doi:10.1016/j.ocemod.2017.12.006.

Gent, P. R., and J. C. McWilliams. 1990. Isopycnal mixing in ocean circulation models. J. Phys. Oceanogr. **20**: 150–155. doi:10.1175/1520-0485(1990)020<0150:IMIOCM>2.0.CO;2.

Gnanadesikan, A. 1999. A simple predictive model for the structure of the oceanic pycnocline. Science **283**: 2077–2079. doi:10.1126/science.283.5410.2077.

Gregory, J. M., K. W. Dixon, R. J. Stouffer, A. J. Weaver, E. Driesschaert, M. Eby, T. Fichefet, H. Hasumi, A. Hu, J. H. Jungclaus, and I. V. Kamenkovich. 2005. A model intercomparison of changes in the Atlantic thermohaline circulation in response to increasing atmospheric CO_2 concentration. Geophys. Res. Lett. **32**: L12703. doi:10.1029/2005GL023209.

Haney, R. L. 1971. Surface thermal boundary condition for ocean circulation models. J. Phys. Oceanogr. **1**: 241–248. doi:10.1175/1520-0485(1971)001<0241:STBCFO>2.0.CO;2.

Held, I. M., and B. J. Soden. 2006. Robust responses of the hydrological cycle to global warming. J. Climate **19**: 5686–5699. doi:10.1175/JCLI3990.1.

Jansen, M. F., L. P. Nadeau, and T. Merlis. 2018. Transient vs. equilibrium response of the ocean's overturning circulation to warming. J. Climate. **31**(13): 5147–5163. doi:10.1175/JCLI-D-17-0797.1.

Jiang, S., P. H. Stone, and P. Malanotte-Rizzoli. 1999. An assessment of the Geophysical Fluid Dynamics Laboratory ocean model with coarse resolution: Annual-mean climatology. J. Geophys. Res. Oceans **104**(C11): 25623–25645. doi:10.1175/JCLI-D-17-0797.1.

Klinger, B. A., and J. Marotzke. 1999. Behavior of double-hemisphere thermohaline flows in a single basin. J. Phys. Oceanogr. **29**(3): 382–399.

Large, W. G., J. C. McWilliams, and S. C. Doney. 1994. Oceanic vertical mixing: A review and a model with a nonlocal boundary layer parameterization. Rev. Geophys. **32**: 363–403. doi:10.1029/94RG01872.

Latif, M. 2000. Tropical stabilization of the thermohaline circulation in a greenhouse warming simulation. J. Climate **13**: 1809–1813. doi:10.1175/1520-0442(2000)013<1809:L>2.0.CO;2.

Lauderdale, J. M. 2010, *On the role of the Southern Ocean in the global carbon cycle and atmospheric CO_2 change*. PhD diss: Univ. of Southampton, UK. doi:10.1007/s10096-010-1042-8.

Levitus, S., and T. Boyer. 1994a, *World Ocean Atlas 1994, volume 3: Salinity*. Washington, D. C.: Tech. Rep., NOAA Atlas NESDIS 3, U.S. Dep. of Commerce.

Levitus, S., and T. Boyer. 1994b, *World Ocean Atlas 1994, Volume 4: Temperature*. Washington, D. C.: Tech. Rep., NOAA Atlas NESDIS 4, U.S. Dep. of Commerce.

Liu, W., S.-P. Xie, Z. Liu, and J. Zhu. 2017. Overlooked possibility of a collapsed Atlantic meridional overturning circulation in warming climate. Sci. Adv. **3**: e1601666. doi:10.1126/sciadv.1601666.

Longworth, H., J. Marotzke, and T. F. Stocker. 2005. Ocean gyres and abrupt change in the thermohaline circulation: A conceptual analysis. J. Climate **18**: 2403–2416. doi:10.1175/JCLI3397.1.

Lumpkin, R., and K. Speer. 2007. Global ocean meridional overturning. J. Phys. Oceanogr. **37**: 2550–2562. doi:10.1175/JPO3130.1.

Marotzke, J. 1994. Ocean models in climate problems, p. 79–109. *In, Ocean processes in climate dynamics: Global and mediterranean examples*. Dordrecht: Springer.

Marshall, J., and K. Speer. 2012. Closure of the meridional overturning circulation through Southern Ocean upwelling. Nat. Geosci. **5**: 171. doi:10.1038/ngeo1391.

Marshall, J., A. Adcroft, C. Hill, L. Perelman, and C. Heisey. 1997. A finite-volume, incompressible Navier Stokes model for studies of the ocean on parallel computers. J. Geophys. Res. Oceans **102**: 5753–5766. doi:10.1029/96JC02775.

Mignac, D., D. Ferreira, and K. Haines. 2019. Decoupled freshwater transport and meridional overturning in the South Atlantic. Geophys. Res. Lett. **46**: 2178–2186. doi:10.1029/2018GL081328.

Nikurashin, M., and G. Vallis. 2012. A theory of the interhemispheric meridional overturning circulation and associated stratification. J. Phys. Oceanogr. **42**: 1652–1667. doi:10.1175/JPO-D-11-0189.1.

Nilsson, J., and G. Walin. 2001. Freshwater forcing as a booster of thermohaline circulation. Tellus A: Dynamic Meteorol. Oceanogr. **53**: 629–641. doi:10.1034/j.1600-0870.2001.00263.x.

Nilsson, J., P. L. Langen, D. Ferreira, and J. Marshall. 2013. Ocean basin geometry and the salinification of the Atlantic Ocean. J. Climate **26**: 6163–6184. doi:10.1175/JCLI-D-12-00358.1.

Rahmstorf, S. 1996. On the freshwater forcing and transport of the Atlantic thermohaline circulation. Climate Dynam. **12**: 799–811. doi:10.1007/s003820050144.

Redi, M. H. 1982. Oceanic isopycnal mixing by coordinate rotation. J. Phys. Oceanogr. **12**: 1154–1158. doi:10.1175/1520-0485(1982)012<1154:OIMBCR>2.0.CO;2.

Rooth, C. 1982. Hydrology and ocean circulation. Prog. Oceanogr. **11**(2): 131–149.

Scott, J. R., J. Marotzke, and P. H. Stone. 1999. Interhemispheric thermohaline circulation in a coupled box model. J. Phys. Oceanogr. **29**: 351–365. doi:10.1175/1520-0485(1999)029<0351:ITCIAC>2.0.CO;2.

Sloss, P. W. 1988, *Data announcement 88-MGG2, digital relief of the surface of the earth*. Boulder, CO: NOAA, Natl. Geophys. Data Cent. doi:10.1126/science.241.4874.1839-a.

Stommel, H. 1961. Thermohaline convection with two stable regimes of flow. Tellus **13**: 224–230. doi:10.3402/tellusb.v13i2.12985.

Stouffer, R. J., and S. Manabe. 2003. Equilibrium response of thermohaline circulation to large changes in atmospheric CO_2 concentration. Climate Dynam. **20**: 759–773. doi:10.1007/s00382-002-0302-4.

Stouffer, R. J., et al. 2006. Investigating the causes of the response of the thermohaline circulation to past and future climate changes. J. Climate **19**: 1365–1387. doi:10.1175/JCLI3689.1.

Straub, D. N. 1996. An inconsistency between two classical models of the ocean buoyancy driven circulation. Tellus A **48**: 477–481. doi:10.1034/j.1600-0870.1996.t01-2-00009.x.

Talley, L. D. 2013. Closure of the global overturning circulation through the Indian, Pacific, and southern oceans: Schematics and transports. Oceanography **26**: 80–97. doi:10.5670/oceanog.2013.07.

Thorpe, R. B., M. Jonathan, T. C. Gregory, R. A. W. Johns, and J. F. B. Mitchell. 2001. Mechanisms determining the Atlantic thermohaline circulation response to greenhouse gas forcing in a non-flux-adjusted coupled climate model. J. Clim. **14**: 3102–3116. doi:10.1175/1520-0442(2001)014<3102:MDTATC>2.0.CO;2.

Trenberth, K., J. Olson, and W. Large. 1989, *A global wind stress climatology based on ECMWF analyses*. *Tech. Rep. NCAR/TN-338+STR*. Boulder, CO: Natl Cent. for Atmos. Res.

Tziperman, E. 2000. Proximity of the present-day thermohaline circulation to an instability threshold. J. Phys. Oceanogr. **30**: 90–104. doi:10.1175/1520-0485(2000)030<0090:POTPDT>2.0.CO;2.

Wang, X., P. H. Stone, and J. Marotzke. 1999. Global thermohaline circulation. Part I: Sensitivity to atmospheric moisture transport. J. Climate **12**: 71–82. doi:10.1175/1520-0442-12.1.71.

Weaver, A. J., J. Marotzke, P. F. Cummins, and E. S. Sarachik. 1993. Stability and variability of the thermohaline circulation. J. Phys. Oceanogr. **23**: 39–60. doi:10.1175/1520-0485(1993)023<0039:SAVOTT>2.0.CO;2.

Welander, P. 1971. The thermocline problem. Phil. Trans. R. Soc. Lond. A **270**: 415–421. doi:10.1098/rsta.1971.0081.

Welander, P. 1986. Thermohaline effects in the ocean circulation and related simple models, p. 163–200. In, Large-scale transport processes in oceans and atmosphere. Dordrecht: Springer.

Wolfe, C. L., and P. Cessi. 2014. Salt feedback in the adiabatic overturning circulation. J. Phys. Oceanogr. **44**: 1175–1194. doi:10.1175/JPO-D-13-0154.1.

Wunsch, C. 2005. Thermohaline loops, Stommel box models and the Sandström theorem. Tellus A **57**: 84–99. doi:10.1111/j.1600-0870.2005.00093.x.

Wunsch, C. 2014, *Modern observational physical oceanography: Understanding the Global Ocean*. Princeton, NJ: Princeton Univ. Press.

Zweng, M. M., J. R. Reagan, J. I. Antonov, R. A. Locarnini, A. V. Mishonov, T. P. Boyer, H. E. Garcia, O. K. Baranova, D. R. Johnson, D. Seidov, and M. M. Biddle. 2013, p. 39. *In* S. Levitus [ed.], *World Ocean Atlas 2013, Volume 2: Salinity*, v. **74**. A. Mishonov Technical Ed.; NOAA Atlas NESDIS.